Materials Science Forum Vols. 738-739 (2013) pp 247-251
Online available since 2013/Jan/25 at www.scientific.net

doi:10.4028/www.scientific.net/MSF.738-739.247

The shape memory effect in melt spun Fe-15Mn-5Si-9Cr-5Ni alloys

DRUKER Ana[1,2,a], LA ROCA Paulo[2,b], VERMAUT Philippe[3,c], OCHIN Patrick[4,d] and MALARRÍA Jorge[1,2,e]

[1]Facultad de Cs. Ex., Ingeniería y Agrimensura (UNR), Av Pellegrini 250, Rosario, Argentina
[2]Instituto de Física Rosario (CONICET-UNR), Bv. 27 de Febrero 210 bis, Rosario, Argentina
[3]Groupe de Métallurgie Structurale, UMR CNRS 70 45, ENSCP, 75231 Paris, France.
[4]Institut de Chimie et des Matériaux Paris-Est, UMR CNRS 7182, 94320 Thiais, France.

[a]ana@asb.com.ar, [b]laroca@ifir-conicet.gov.ar, [c]philippe-vermaut@chimie-paristech.fr, [d]ochin@icmpe.cnrs.fr, [e]malarria@ifir-conicet.gov.ar

Keywords: shape memory, Fe-Mn-Si, melt-spun.

Abstract. At room temperature, Fe-15Mn-5Si-9Cr-5Ni alloys are usually austenitic and the application of a stress induces a reversible martensitic transformation leading to a shape memory effect (SME). However, when a ribbon of this material is obtained by melt-spinning, the rapid solidification stabilizes a high-temperature ferritic phase. The goals of this work were to find the appropriate heat treatment in order to recover the equilibrium austenitic phase, characterize the ribbon form of this material and evaluate its shape memory behaviour. We found that annealing at 1050ºC for 60 min, under a protective argon atmosphere, followed by a water quenching stabilizes the austenite to room temperature. The yield stress, measured by tensile tests, is 250 MPa. Shape-memory tests show that a strain recovery of 55% can be obtained, which is enough for certain applications.

Introduction

Deformation of the Fe–Mn–Si-based alloy induces a hexagonal ε martensite from a fcc γ austenite. This martensite is produced by the formation and overlapping of stacking faults in the parent phase, and if heated, it can revert back to the austenite. This is the principle behind the alloy's shape-memory properties [1]. Although many alternative techniques have been used to optimize the shape-memory effect in Fe–Mn–Si based alloys [2, 3], rolling and annealing were found to be one of the more convenient method of processing. The rolling and annealing technique also lends itself to large-scale industrial production [4, 5]. Such processing produces an alloy with fine austenitic grains and the appropriate microstructure.

Rapid solidification of shape-memory ferrous-based alloys has received limited attention, although this field of study is relevant to the production, as well as to the welding of these materials. Following Herrera et al. [6], the use of melt spinning as an investigative tool, permits good control of the cooling rates, and provides the opportunity to control and understand the microstructure of the alloys. Ribbons produced by melt spinning consist of columnar grains growing from the chill zone, which is the spinning-wheel surface. Donner et al. [7] began researching various Fe-(24-30)Mn-(2.6-4.7)Si alloys in 1989, and many years later Valeanu et al. [8] focused their studies on the magnetic behaviour of these materials.

Our work centred on characterizing the microstructure and properties of Fe-15Mn-5Si-9Cr-5Ni melt-spun, shape-memory alloy ribbons after casting and heat treatments. We compared these materials to ones from the same batch produced by conventional rolling processes, evaluating the martensitic transformation and shape-memory properties.

Experimental procedures

We have produced rapidly solidified ribbons of Fe-15Mn-5Si-9Cr-5Ni, approximately 10 x 0.030 mm in cross section, in a helium atmosphere by a planar flow-casting process. The base material was prepared initially by melting commercial-quality materials and casting in a sand mould. Small pieces of these ingots were melted by induction heating in a quartz crucible and then ejected with a

200 mbar argon flux onto a copper wheel. The quartz crucible had a nozzle slit of 0.3 mm and the crucible to substrate gap was 0.2 mm. The wheel speed and temperature were 20 m/s and 25º C, respectively. After casting, samples were heat treated in an argon atmosphere and quenched in water, as summarized in Table 1. To identify and quantify the phases we performed X-ray diffraction with a Philips X-pert pro goniometer. Microstructural analysis was performed with an Olympus PME3 (OM) equipped with a NIC device, a FEI Quanta 200 (SEM), and a Philips EM300 (TEM). TEM specimens were electropolished using the double-jet thinning technique in a 90/10 (vol. %) acetic/perchloric solution at room temperature. To evaluate the mechanical and shape-memory properties, we performed thermal cycling tests in a home-made device adapted from a creep-test machine, and tensile tests in an Instron 3362 universal machine. The reverse transformation was induced by heating the samples above the final reversion A_f temperature.

Table 1: Heat treatments applied to ribbon **P**

P 6	Annealed at 650º C for 30 min
P 9	Annealed at 1000º C for 10 min
P 10	Annealed at 1050º C for 60 min
P 11	Annealed at 1050º C for 120 min

Results and discussion

The rolled alloy. We investigated an alloy rolled from ingots prepared under conditions reproducible at the industrial level [5, 9]. Among the different thermo-mechanical treatments applied to the samples, a final rolling stage to 35% thickness reduction at 800º C followed by annealing at 650º C, lead to the best behaviour. Samples of this material recover around 92 % of a 2.6 % tensile deformation and 96 % of a 2.5 % bending deformation. The stress which activates the $\gamma \rightarrow \varepsilon$ martensitic transformation is 450 MPa. This behaviour is due to a microstructure that optimizes the nucleation and growth of fine martensitic plates, a morphology that promotes the $\varepsilon \rightarrow \gamma$ reverse transformation to take place by inverting the crystalline path followed in the direct stress-induced transformation. X-ray diffraction reveals an almost complete austenite phase and few $Fe_5Ni_3Si_2$ precipitates [10]. On the other hand, the sheets rolled at 800º C and annealed at 1000º C transform at 360 MPa and recover 55 % of 3 % induced deformation.

Images obtained using OM and TEM show a marked contrast between sheets annealed at 650º C and 1000º C, even though both specimens were rolled at 800º C. Annealing at 650º C produces some precipitates at the grain and twin boundaries (Fig. 1a), while the average grain size is 27 μm. The annealing at 1000º C gives well-defined grains, of 62 μm characteristic size (Fig. 1c). In both conditions, deformation twins were observed. This is a common feature in low SFE alloys. TEM image in Fig. 1b shows a high density of stacking faults and perfect dislocations in the material rolled at 800º C and annealed at 650º C; this condition provides enough hardness in the austenite phase to promote the stress-induced martensitic transformation instead of plastic deformation. Annealing at 1000º C (Fig. 1d) activates the recrystallization process; the result is the nucleation and growth of dislocation-free austenitic grains, with only a medium density of stacking faults.

The as-cast ribbon. A ribbon thickness of 0.030 mm was measured with a micrometer, and we used this value for stress calculations. Nevertheless, SEM observations show that the cross sectional thickness is actually non uniform, reaching lower values of about 0.012 mm at depressed thickness zones of the ribbons. Thus, characteristic stress values of the ribbons mentioned hereafter might be underestimated. Other irregularities, like pockets and edge serrations, may produce stress concentrations and brittleness, also influencing the tensile-test results.

We found through X-ray diffraction studies, that mainly the BCC phase (δ ferrite) is present at room temperature. This should be expected in this alloy, which contains elements that simultaneously stabilize the FCC (γ austenite) and BCC phases. The presence of a single phase or both, irrespective of proportion, depends on the solidification velocity. The process conditions des-

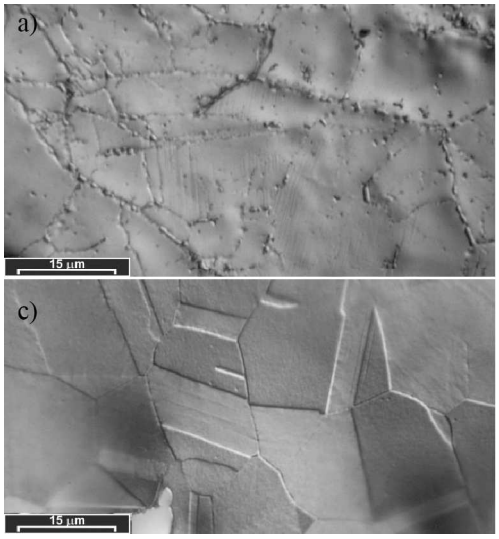

Fig. 1: Microstructure obtained by rolling at 800ºC annealed in two conditions: a) (OM) annealed at 650ºC present grain size of 27 um, twins in the austenitic matrix and some precipitates in grain boundaries and twins boundaries, b) TEM images shows a high density of stacking faults and perfect dislocations (zone axis $[110]_{FCC}$), c) (OM) annealed at 1000ºC result in grain sizes of 62 υm and deformation twins, d) zone axis $[112]_{FCC}$ BF TEM image shows that dislocations are no longer present in the austenite.

cribed above produced very thin ribbons, so that the interfacial heat-transfer coefficient dominates in establishing the quench rate. As a consequence, a thinner thickness indicates a higher cooling rate, and this influences not only which phase is retained at room temperature, ferrite in our case, but the dendritic microstructure, as well.

Heat treatments. Since the SME is the result of the reversible γ↔ε martensitic transformation, the presence of ferrite is undesirable. So, we tried several heat treatments to obtain austenite at room temperature. Fig. 2 depicts the evolution of the phases. Ribbon **P**, in the as melt-spun condition, has only 3 % of the γ phase. **P6** shows that annealing at 650º C for 30 min. transforms 33 % of the δ phase to γ (value estimated from the intensity of the $(111)_{FCC}$, $(200)_{FCC}$ and $(220)_{FCC}$ peaks), and promotes the incipient precipitation of $Fe_5Ni_3Si_2$ [10] that we estimate to be about 3-4 vol. %. The crystal structure of this compound is cubic, belonging to the space group $P2_13$ (198). The OM image in Fig. 3a shows that the grain size is about 4 µm. **P9**, **P10** and **P11** correspond to treatments at 1000º C for 10 min, 1050º C for 60 min and 1050º C for 120 min, respectively. The second treatment gives a completely austenitic structure at room temperature, with a grain size of 15 µm (see SEM image in Fig. 3b). If the time is increased to 120 min at 1050º C, ribbon **P11**, the austenitic grain size grows to 30 µm (Fig. 3c). This leads to an increase of the M_s temperature [11]. The consequent proportion of thermal ε martensite formed during cooling, adversely affects the reversibility of the subsequent stress-induced martensite, because the latter grows from the pre-existing martensite, generating large plates. Finally, we found that annealing at 1050º C for 60 min is the most appropriate heat treatment for retaining austenite at room temperature.

When samples for TEM observations were prepared, the double-jet polishing acted preferentially in the thinnest areas, i.e. around pockets and depressed thickness zones. The image of sample **P10**, annealed at 1050º C for 60 min., shows a medium density of stacking faults on {111}

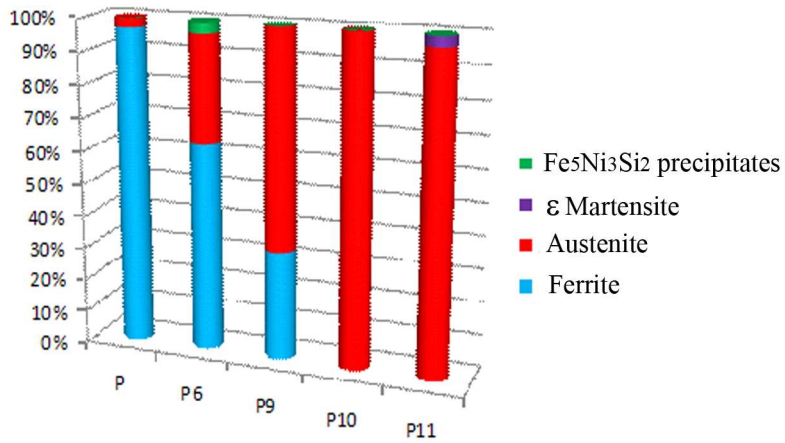

Fig. 2: Phase proportions detected in ribbon P, as cast, and after the heat treatments described in Table 1.

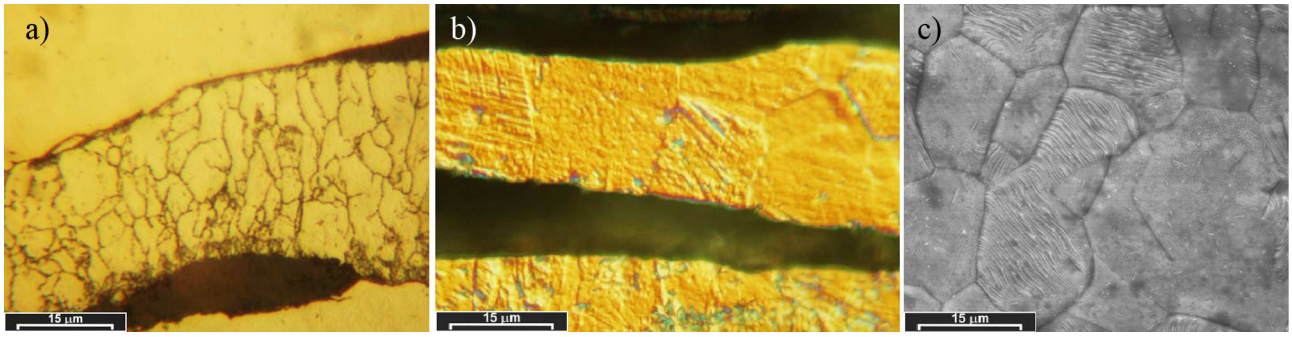

Fig. 3: Microstructure obtained from different annealings of ribbon **P**: a) at 650º C for 30 min (**P6**); b) at 1050º C for 60 min (**P10**); c) at 1050º C for 120 min (**P11**).

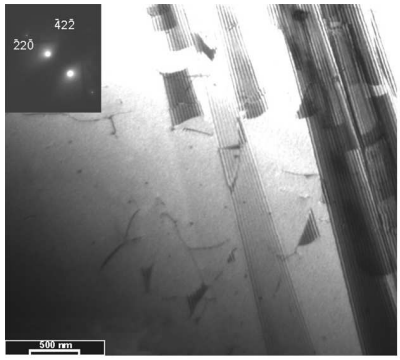

Fig. 4: Microstructure obtained by annealing at 1050º C for 60 min (**P10**).

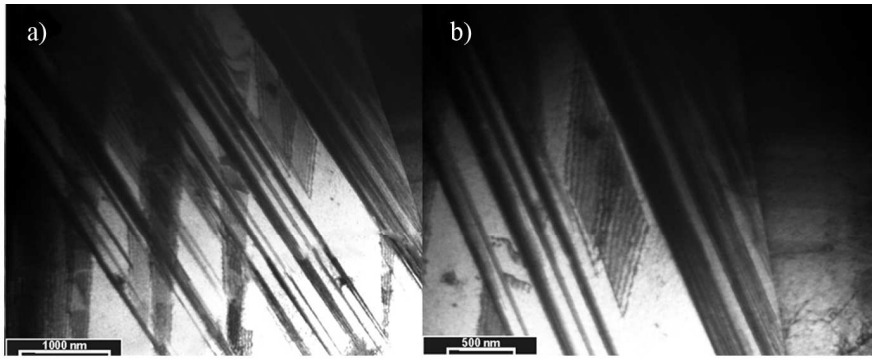

Fig. 5: a) ribbon **P10** tensile tested presents parallel martensite plates; b) higher magnification shows a fine distribution of plates growing into the ε plates.

planes and few dislocations in the austenitic grains, Fig. 4. The similarity is remarkable between this microstructure and that observed for the sheets rolled at 800º C and annealed at 1000º C.

Martensitic transformation and shape-memory tests. Samples taken from ribbon **P10** were tensile tested at room temperature with two aims: first, to determinate the value of the stress that activates the $\gamma \rightarrow \varepsilon$ transformation, $\sigma_{\gamma \rightarrow \varepsilon}$; and second, to observe the obtained martensite in the TEM. The $\sigma_{\gamma \rightarrow \varepsilon}$ measured transformation stress was 230-270 MPa. This is perhaps a slight underestimated, because of the non-homogeneous ribbons' cross-section described above. Fig. 5 shows TEM images. Martensite seems to be in an almost edge-on condition; plates are rather thin – only one {111} austenitic plane thick – and parallel. Moreover, Fig. 5b permits identification of a fine distribution of plates growing into the ε plates observed in Fig. 5a. Tensile tests to 3% elongation followed by heating to 550º C for 20 min, were performed to determinate the ribbons' shape-memory behaviour. Before testing, we marked the specimens' surfaces. The degree of shape recovery (*DSR)* of the **P10** specimens was 52 %. Another test was performed to allow us to draw the strain-temperature curve shown in Fig. 6 and thus, to evaluate the amount of deformation associated with the martensitic transformation. In the first stage, we applied a stress of 300 MPa (a value taken from the previous tests) to induce the martensitic transformation at room temperature; the deformation achieved was 5%. During the subsequent unloading, an elastic recovery (ε_{elas}) of about 1 % occurred. Then, the sample was slowly heated over a temperature range from 20 to 350º C. It is notable that the $\varepsilon \rightarrow \gamma$ inverse transformation began at 50º C, while the plateau was reached at about 240º C, indicating that the A_f temperature was attained. During cooling, the material contracted. The remnant deformation was 1.8 %, resulting in a shape recovery of 55 %.

Although the martensite morphology corresponds to a condition favourable for obtaining a large SME, the matrix could possibly be deforming plastically, resulting in a ribbons with a SME just above 50 %. The absence of perfect dislocations softens the austenite, while its grain size allows the martensite plates to grow over large distances without being stopped by grain boundaries.

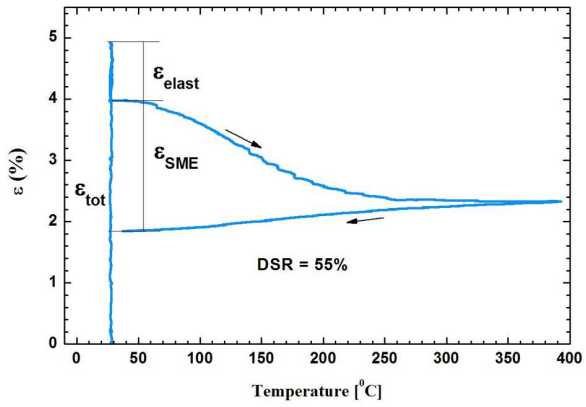

Fig. 6: Thermal cycling under a constant load to determine shape recovery.

Conclusions

We have prepared ribbons of Fe-15Mn-5Si-9Cr-5Ni shape-memory alloy by the melt-spinning technique. The rapid solidification produced the undesirable δ ferrite phase, but annealing at 1050º C for 60 min. transforms the ferrite to austenite, which is completely retained upon cooling to room temperature. The result is an almost dislocation-free microstructure, containing a medium density of stacking faults. Although the martensite induced by an applied deformation has the correct morphology for the shape recovery, the tests showed a value of around 50 %. Similar results have been measured for sheets rolled at 800º C and annealed at 1000º C, a treatment which produces a microstructure similar to that of the ribbons.

Currently, we are fabricating new ribbons prepared under different processing conditions. This material seems to be austenitic at room temperature, demonstrating that it is possible to obtain Fe-based shape-memory ribbons in a single step.

References

[1] Sato A., Chishima E., Soma K., Mori T. Shape memory effect in γ↔ε transformation in Fe-30Mn-1Si alloy single crystals. Acta Metall. 30 (1982) 1177-1183.

[2] H. Otsuka, M. Murakami, S. Matsuda, in: M. Doyama, S. Somiya, R. Chang (Eds.), Proceedings of the MRS International Meeting on Advanced Materials, vol. 9, Materials Research Society (1988) 451–456.

[3] Kajiwara S. Characteristic features of shape memory effect and related transformation behavior in Fe-based alloys. Mater. Sci. Eng. A 67 (1999) 273–275.

[4] Stanford N., Dunne D.P. Effect of NbC and TiC precipitation on shape memory in an iron-based alloy. J. Mater. Sci. 41 (2006) 4883-4891.

[5] Druker A., Sobrero C., Brokmeier H.-G., Malarría J., Bolmaro R. Texture evolution during thermomech. treatments in Fe-Mn-Si shape memory alloys. Mater. Sci. Eng. A 481–482 (2008) 578–581.

[6] Herrera C., de Lima N.B., Kliauga A.M., Padilha A.F. Microstructure and texture of duplex stainless steel after melt-spinning processing. Mater. Charact. 59 (2008) 79–83

[7] Donner P., Hornbogen E., Sade M. Shape memory effects in melt-spun Fe-Mn-Si alloys. J. Mater. Sci. Lett. 8 (1989) 37-40.

[8] Valeanu M., Filoti G., Kuncser V., Tolea F., Popescu B., Galatanu A., Schinteie G., Jianu A.D., Mitelea I., Schinle D., Craciunescu C.M. Shape memory and associated properties in Fe–Mn–Si-based ribbons produced by melt-spinning. J. Mag. Magnetic Mater. 320 (2008) e164–e167.

[9] Druker A., Perotti A., Baruj A., Malarría J. Heat Treatments of Fe-Mn-Si Based Alloys: Mechanical Properties and Related Shape Memory Phenomena. J. ASTM Int. 8, No. 4 (2011) Paper ID JAI103399. Available online at www.astm.org

[10] Maji B., Madangopal K, Rama Rao V. V. The microstructure of an Fe-Mn-Si-Cr-Ni stainless steel shape memory alloy. Met. Mater. Trans. A 34a (2003) 1029-1042.

[11] Jiang B.H., Sun L., Li R., Hsu T.Y. Influence of austenite grain size on γ→ε martensitic transformation temperature in Fe-Mn-Si-Cr. Scr. Met. et Mater. 33 (1995) 63-68.

European Symposium on Martensitic Transformations
10.4028/www.scientific.net/MSF.738-739

The Shape Memory Effect in Melt Spun Fe-15Mn-5Si-9Cr-5Ni Alloys
10.4028/www.scientific.net/MSF.738-739.247